

Detailed Spectroscopic and Photometric Analysis of DQ White Dwarfs

P. Dufour, P. Bergeron, and G. Fontaine

*Département de Physique, Université de Montréal, C.P. 6128, Succ.
Centre-Ville, Montréal, Québec, Canada, H3C 3J7*

Abstract. We present an analysis of spectroscopic and photometric data for cool DQ white dwarfs based on improved model atmosphere calculations. In particular, we revise the atmospheric parameters of the trigonometric parallax sample of Bergeron et al. (2001), and discuss the astrophysical implications on the temperature scale and mean mass, as well as the chemical evolution of these stars. We also analyze 40 new DQ stars discovered in the first data release of the Sloan Digital Sky Survey.

1. Introduction

Cool white dwarfs showing traces of carbon, either as neutral carbon lines or molecular C₂ Swan bands, are collectively known as DQ stars. Past analyses showed that these stars are helium rich with carbon abundances ranging from $\log C/He = -7$ to -2 as determined from optical or ultraviolet (IUE) spectroscopic observations (Bues 1973; Grenfell 1974; Koester et al. 1982; Wegner & Yackovich 1984; Weidemann & Koester 1995).

The presence of carbon has been successfully explained by a model in which carbon diffusing upward from the core is brought to the photosphere by the deep helium convection zone (Pelletier et al. 1986). This model was shown to reproduce the observed carbon abundance distribution as a function of effective temperature fairly well for a helium layer thickness of $\log q(He) \equiv M_{He}/M_{\star} \sim -3.75$, a value at odds with those obtained from evolutionary models of post-AGB stars that predict much thicker helium layers of the order of $\log q(He) \sim -2$.

More recently, Bergeron et al. (1997) and Bergeron et al. (2001, hereafter collectively referred to as BLR) presented a photometric and spectroscopic analysis of a large sample of white dwarfs aimed at improving our understanding of the chemical evolution of cool white dwarfs. Their sample includes several DQ stars that were analyzed with pure-helium model atmospheres, the only models available at that time. Recently, Provencal et al. (2002) studied the importance of including carbon in the atmospheres of the DQ star Procyon B. Their effective temperature of $T_{\text{eff}} = 7740 \pm 50$ K, derived from models including carbon, was significantly cooler than the earlier value of $T_{\text{eff}} = 8688 \pm 200$ K obtained by Provencal et al. (1997) on the basis of pure helium models. This large difference was attributed to an increase of the He⁻ free-free opacity resulting from the additional free electrons provided by carbon.

The natural step following the comprehensive studies of BLR is thus to include explicitly metals and molecules in the model atmospheres.

2. Theoretical Framework

The model atmosphere code is a modified version of that described at length in Bergeron et al. (1995), which is appropriate for pure hydrogen and pure helium atmospheric compositions, as well as mixed hydrogen and helium compositions. In order to treat in detail white dwarfs of the DQ and DZ spectral types, we had to include metals and molecules in our equation-of-state and opacity calculations. Details will be provided elsewhere (Dufour et al. 2005, in preparation). Since in this analysis we are only concerned with DQ stars showing the C₂ Swan bands, we need only to include helium and carbon. Our model grid covers a range of $T_{\text{eff}} = 5000$ to 12,000 K in steps of 500 K, $\log g = 7.5$ to 9.5 in steps of 0.5 dex, and $\log C/\text{He} = -9.0$ to -2.0 in steps of 0.5 dex.

3. Analysis of the BLR Sample

The first sample used for this study is drawn from the BLR analysis. It consists of 12 DQ stars with trigonometric parallax measurements, high signal-to-noise spectroscopy showing the carbon molecular bands, optical *BVRI* and infrared *JHK* photometry. The method used to fit the data is similar to that described at length in BLR, with the exception that in addition to the effective temperature and the solid angle $\pi(R/D)^2$, we now have a third fitting parameter, the carbon abundance. Briefly, we transform the magnitudes at each bandpass into average fluxes. The resulting energy distributions are then fitted with the model fluxes, properly averaged over the filter bandpasses, using a nonlinear least-squares method.

We begin by assuming a pure helium composition and $\log g = 8.0$ to get initial estimates of T_{eff} and $\pi(R/D)^2$. The solid angle is combined with the distance D derived from the trigonometric parallax to obtain the stellar radius R . This radius is then converted into $\log g$ using an appropriate mass-radius relation for white dwarfs, and the procedure is repeated until a convergence in $\log g$ is reached. Next we turn to the spectroscopic observations and determine the carbon abundance by fitting the Swan bands at the values of T_{eff} and $\log g$ obtained from the fit to the energy distribution. This carbon abundance is then used to obtain new estimates of the atmospheric parameters from the energy distribution, and so forth. We repeat the procedure — typically five iterations — until T_{eff} , $\log g$, and the carbon abundance converge to a consistent photometric and spectroscopic solution. The $\log g$ values are then converted into masses using the cooling models of Fontaine et al. (2001).

Our spectroscopic fits for the BLR sample are displayed in Figure 1; the photometric fits differ very little from those already shown in BLR and will thus not be repeated here.

We compare in Figure 2 the effective temperatures and masses derived from pure helium models (e.g. BLR) with those obtained here with models including carbon (see also Weidemann, these proceedings). We find that our revised effective temperatures are reduced significantly with respect to the pure helium

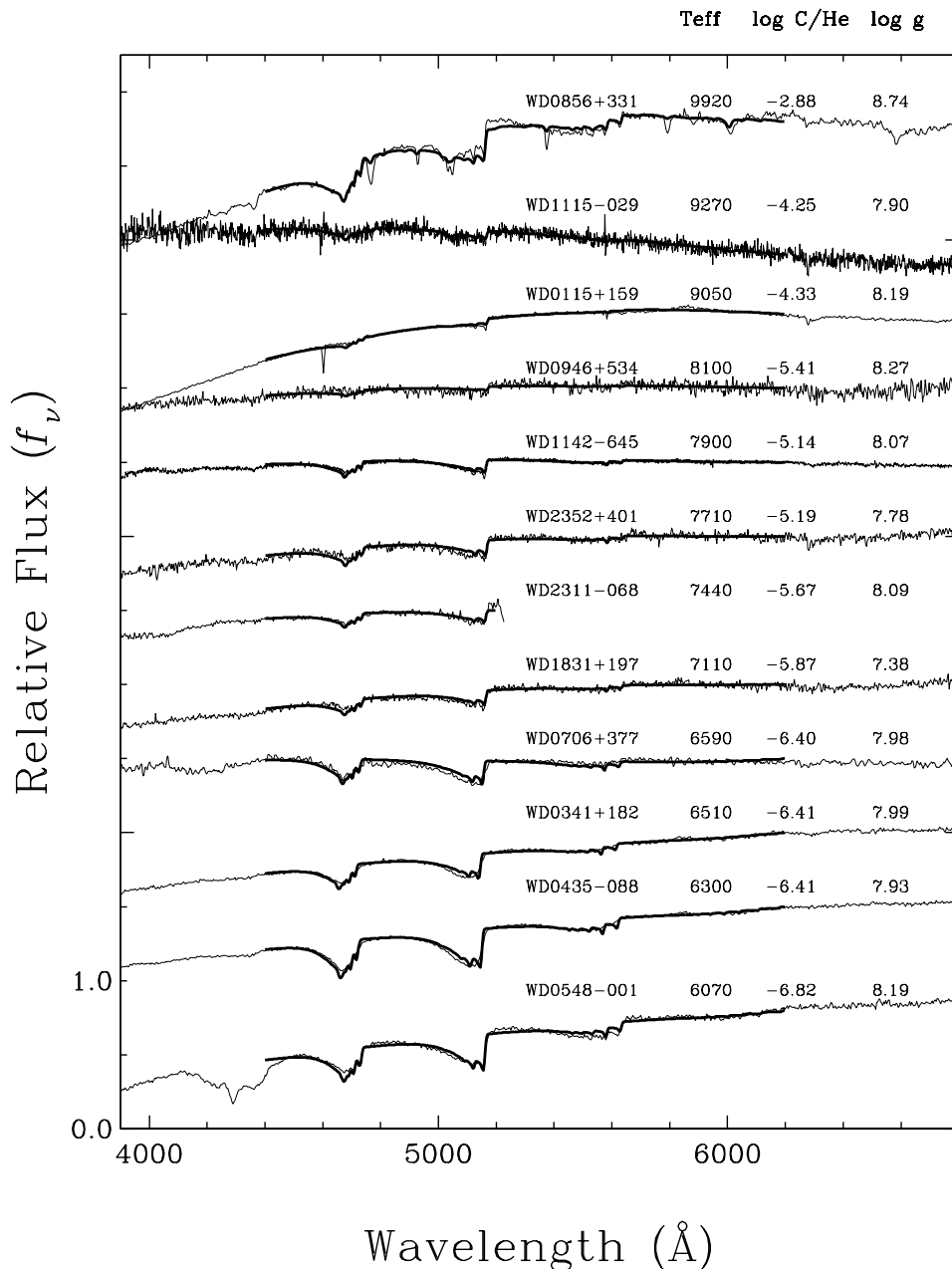


Figure 1. Fits to the Swan bands plotted in order of decreasing temperatures from top to bottom. WD 0856+331 also shows atomic C I lines.

solutions, in agreement with the conclusions of Provencal et al. (2002) for Procyon B. The inclusion of carbon in the equation-of-state increases the number of free electrons and consequently the contribution of the He^- free-free opacity. The resulting effects on the atmospheric structures can produce significant dif-

ferences in the derived atmospheric parameters. Since the T_{eff} values have been greatly reduced, so are the model fluxes, and larger solid angles are required to fit the photometric data, which imply larger stellar radii or smaller masses, as shown in Figure 2.

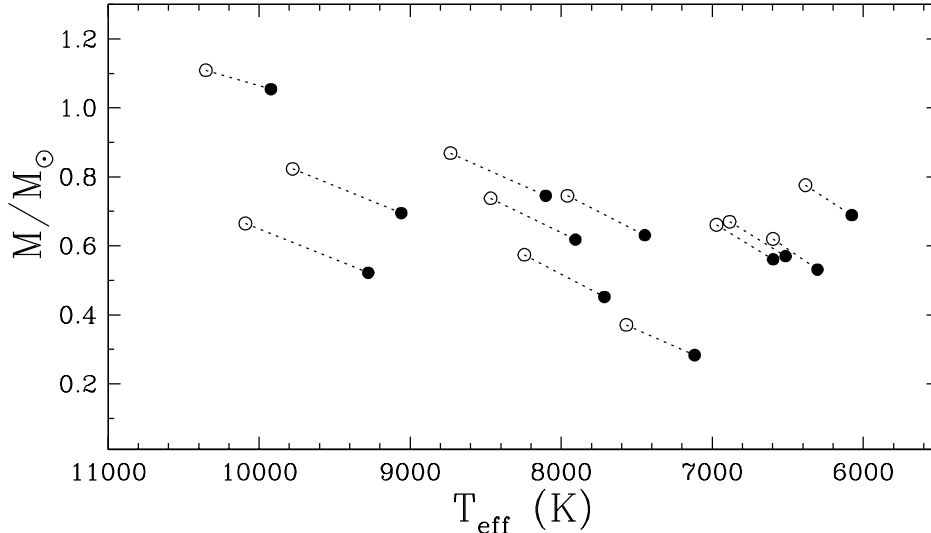


Figure 2. Comparison of effective temperatures and masses obtained from pure helium models (*open circles*) and models including carbon (*filled circles*).

An interesting consequence of our findings concerns the mass distribution of DQ stars. An intriguing question raised by BLR was the fact that the mean mass of DQ stars, $\langle M \rangle = 0.72 M_{\odot}$, was much higher than that obtained for their likely progenitors, the DB stars, by Beauchamp et al. (1996), $\langle M \rangle = 0.59 M_{\odot}$, based on spectroscopic fits. Our improved analysis brings the mean mass of DQ stars down to $\langle M \rangle = 0.61 M_{\odot}$, in much better agreement with the spectroscopic mean mass of DB stars, and more in line with our understanding of white dwarf evolution.

4. Analysis of the SDSS Sample

Our second sample consists of 40 stars spectroscopically identified as DQ (human ID) in the first data release of the Sloan Digital Sky Survey (SDSS). Details concerning these observations are described in Kleinman et al. (2004) and references therein. Prior to the SDSS study, only 37 cool ($T_{\text{eff}} < 15,000$ K) white dwarfs with carbon features had been analyzed by various investigators, and the SDSS first data release *alone* has more than doubled the number of DQ stars known, allowing us to improve significantly the statistics of DQ stars. The method we use here to fit the SDSS data is similar to that described above, with the exception that the SDSS *ugriz* photometry is used instead. These photometric passbands cover the entire optical range from the UV atmospheric cutoff (3200 Å) to the red sensitivity cutoff of the detector ($\sim 10,000$ Å). Furthermore,

since trigonometric parallax measurements are not available for the SDSS stars, we assume a value of $\log g = 8.0$ for all objects.

5. Discussion

Our results are summarized in Figure 3 where we show the carbon abundances as a function of T_{eff} for both the BLR and SDSS samples. We see that the carbon abundances form a relatively narrow sequence in the $\log C/\text{He} - T_{\text{eff}}$ plane. The sequence defined by the SDSS sample overlaps the BLR sequence quite nicely, suggesting that the physical characteristics of these two samples are very similar. Since the BLR sample as a whole has a normal mean mass near $0.6 M_{\odot}$, the value of $\log g = 8$ assumed for the SDSS sample is probably reasonable. It is also comforting to see that Procyon B (star symbol at 7740 K), with a precise mass determination of $0.602 M_{\odot}$ determined by Provencal et al. (2002), falls well within our sequence. Our results are thus entirely consistent with the idea that all DQ stars evolved from hotter DB white dwarfs.

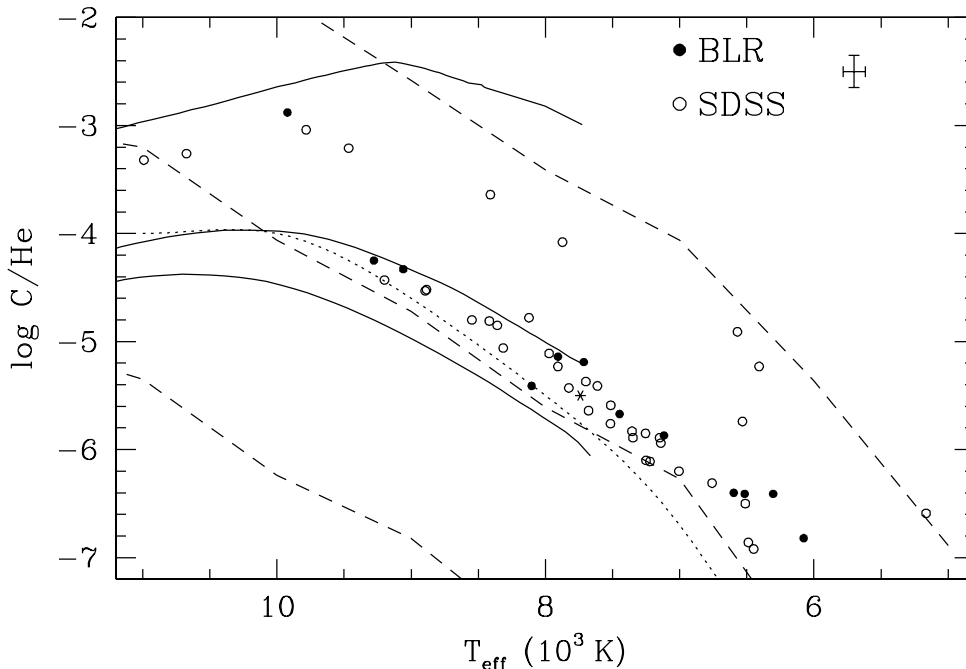


Figure 3. Observed carbon abundances as a function of T_{eff} for both the BLR sample (*filled circles*) and SDSS sample (*open circles*); the star symbol shows the location of Procyon B. The error bars in the upper right corner indicate the average uncertainties of T_{eff} (~ 150 K) and $\log C/\text{He}$ (~ 0.3 dex). The dotted line represents our detection threshold for the C_2 Swan bands (or atomic C I lines for $T_{\text{eff}} > 10,000$ K). The solid and dashed curves correspond to the evolutionary sequences discussed in the text.

Also shown in Figure 3 are the results from two different sets of evolutionary model calculations, which predict the carbon abundances as a function of decreasing effective temperatures for various values of the thickness of the he-

lium layer $q(\text{He})$. The dashed curves represent the calculations of Pelletier et al. (1986) at $0.6 M_{\odot}$ with, from top to bottom, $\log q(\text{He}) = -4.0$, -3.5 , and -3.0 . As discussed in the Introduction, our abundance determinations would suggest values of $\log q(\text{He})$ smaller than -3.5 for all DQ stars, much thinner than the values predicted by post-AGB evolutionary models. A new generation of evolutionary models computed by Fontaine & Brassard (these proceedings) yield quite different results, however, as shown in Figure 3 by the solid curves for models at $0.6 M_{\odot}$ with, from top to bottom, $\log q(\text{He}) = -4.0$, -3.0 , and -2.0 . With these new models, the observed carbon abundances in DQ stars are consistent with values of the helium layer thickness between $\log q(\text{He}) = -3$ and -2 , in much better agreement with the results from post-AGB models.

Several objects in Figure 3 show carbon abundances that lie about 1 dex above the bulk of DQ stars. Among these, the only white dwarf with a measured trigonometric parallax is G47-18 (WD 0856+331; top filled circle) with an estimated mass of $M = 1.05 M_{\odot}$, by far the most massive DQ star in Figure 1. It is thus tantalizing to suggest that the DQ stars with larger-than-average carbon abundances represent the high mass component of the white dwarf mass distribution. Liebert et al. (2003) has suggested that the hot DQ stars discovered in the SDSS could all be massive, and could correspond to the missing high mass tail of the DB star mass distribution (Beauchamp et al. 1996). If both hypotheses are confirmed, the cool DQ stars with large carbon abundances observed here would simply represent the natural extension of the hot DQ stars identified by Liebert et al. Finally, the absence of neutral carbon lines in the optical spectra of DB stars with normal masses is naturally explained by our results. Indeed, the expected carbon abundances in hot ($T_{\text{eff}} > 10,000$ K) helium-rich white dwarfs with $\log q(\text{He})$ between -3 and -2 fall below the detection threshold of the atomic C I lines according to Figure 3.

This work was supported in part by the NSERC Canada and by the Fund FQRNT (Québec).

References

- Beauchamp, A., Wesemael, F., Bergeron, P., Liebert, J., & Saffer, R. A. 1996, ASP Conf. Ser. 96: Hydrogen Deficient Stars, 295
- Bergeron, P., Leggett, S. K., & Ruiz, M. T. 2001, ApJS, 133, 413
- Bergeron, P., Ruiz, M. T., & Leggett, S. K. 1997, ApJS, 108, 339
- Bergeron, P., Saumon, D., & Wesemael, F. 1995, ApJ, 443, 764
- Bues, I. 1973, A&A, 28, 181
- Fontaine, G., Brassard, P., & Bergeron, P. 2001, PASP, 113, 409
- Grenfell, T. C. 1974, A&A, 31, 303
- Kleinman, S. J., et al. 2004, ApJ, 607, 426
- Koester, D., Weidemann, V., & Zeidler, E.-M. 1982, A&A, 116, 147
- Liebert, J., Harris, H. C., Schmidt, G. D., et al. 2003, AJ, 126, 2521
- Pelletier, C., Fontaine, G., Wesemael, F., Michaud, G., & Wegner, G. 1986, ApJ, 307, 242
- Provencal, J. L., Shipman, H. L., Koester, D., Wesemael, F., & Bergeron, P. 2002, ApJ, 568, 324
- Provencal, J. L., Shipman, H. L., Wesemael, F., Bergeron, P., Bond, H. E., Liebert, J., & Sion, E. M. 1997, ApJ, 480, 777
- Wegner, G. & Yackovich, F. H. 1984, ApJ, 284, 257
- Weidemann, V. & Koester, D. 1995, A&A, 297, 216